

# Rapid *in situ* diversification rates in Rhamnaceae explain the parallel evolution of high diversity in temperate biomes from global to local scales

Qin Tian<sup>1,2,3,4</sup> , Gregory W. Stull<sup>1</sup> , Jürgen Kellermann<sup>5,6</sup> , Diego Medan<sup>7</sup>, Francis J. Nge<sup>5,6,8</sup> , Shui-Yin Liu<sup>1,2,3</sup> , Heather R. Kates<sup>9</sup>, Douglas E. Soltis<sup>9,10</sup> , Pamela S. Soltis<sup>9</sup> , Robert P. Guralnick<sup>9</sup> , Ryan A. Folk<sup>11</sup> , Renske E. Onstein<sup>4,12,13\*</sup>  and Ting-Shuang Yi<sup>1,2,3\*</sup> 

<sup>1</sup>Germplasm Bank of Wild Species, Yunnan Key Laboratory of Crop Wild Relatives Omics, Kunming Institute of Botany, Chinese Academy of Sciences, Kunming, 650201, China; <sup>2</sup>University of Chinese Academy of Sciences, Beijing, 101408, China; <sup>3</sup>Key Laboratory of Plant Diversity and Specialty Crops, Chinese Academy of Sciences, Beijing, 100093, China; <sup>4</sup>Naturalis Biodiversity Center, Darwinweg 2, 2333CR, Leiden, the Netherlands; <sup>5</sup>State Herbarium of South Australia, Botanic Gardens and State Herbarium, Hackney Road, Adelaide, SA, 5000, Australia; <sup>6</sup>School of Biological Sciences, The University of Adelaide, Adelaide, SA, 5005, Australia; <sup>7</sup>Cátedra de Botánica General, Facultad de Agronomía, Universidad de Buenos Aires, Ave San Martín 4453, C1417DSE, Buenos Aires, Argentina; <sup>8</sup>IRD – Institut de Recherche pour le Développement, Ave Agropolis BP 64501, Montpellier, 34394, France; <sup>9</sup>Florida Museum of Natural History, University of Florida, Gainesville, FL 32611, USA; <sup>10</sup>Department of Biology, University of Florida, Gainesville, FL 32611, USA; <sup>11</sup>Department of Biological Sciences, Mississippi State University, Mississippi, MS 39762, USA; <sup>12</sup>Evolution and Adaptation, German Centre for Integrative Biodiversity Research (iDiv) Halle–Jena–Leipzig, Puschstrasse 4, Leipzig, 04103, Germany; <sup>13</sup>Leipzig University, Leipzig, 04013, Germany

## Summary

Authors for correspondence:  
Renske E. Onstein  
Email: [onsteinre@gmail.com](mailto:onsteinre@gmail.com)

Ting-Shuang Yi  
Email: [tingshuangyi@mail.kib.ac.cn](mailto:tingshuangyi@mail.kib.ac.cn)

Received: 27 August 2023  
Accepted: 20 November 2023

*New Phytologist* (2024) **241**: 1851–1865  
doi: 10.1111/nph.19504

**Key words:** biodiversity hotspot, macroevolution, Mediterranean-type ecosystem, niche conservatism, phylogenomics, Rhamnaceae, species richness, time-for-speciation.

- The macroevolutionary processes that have shaped biodiversity across the temperate realm remain poorly understood and may have resulted from evolutionary dynamics related to diversification rates, dispersal rates, and colonization times, closely coupled with Cenozoic climate change.
- We integrated phylogenomic, environmental ordination, and macroevolutionary analyses for the cosmopolitan angiosperm family Rhamnaceae to disentangle the evolutionary processes that have contributed to high species diversity within and across temperate biomes.
- Our results show independent colonization of environmentally similar but geographically separated temperate regions mainly during the Oligocene, consistent with the global expansion of temperate biomes. High global, regional, and local temperate diversity was the result of high *in situ* diversification rates, rather than high immigration rates or accumulation time, except for Southern China, which was colonized much earlier than the other regions. The relatively common lineage dispersals out of temperate hotspots highlight strong source-sink dynamics across the cosmopolitan distribution of Rhamnaceae.
- The proliferation of temperate environments since the Oligocene may have provided the ecological opportunity for rapid *in situ* diversification of Rhamnaceae across the temperate realm. Our study illustrates the importance of high *in situ* diversification rates for the establishment of modern temperate biomes and biodiversity hotspots across spatial scales.

## Introduction

Understanding the historical processes responsible for heterogeneity in the distribution of species richness across the globe is a major goal in evolutionary biology (Schluter & Pennell, 2017). The most prominent diversity pattern at the global scale is the tendency for species richness to increase toward the equator, that is the latitudinal diversity gradient (Hillebrand, 2004; Jablonski *et al.*, 2006; Mittelbach *et al.*, 2007). However, deviations from this global pattern, such as the high species richness and

endemism in temperate biomes (i.e. bimodal latitudinal diversity gradient) rather than tropical biomes, remain puzzling (Orr *et al.*, 2021). Indeed, one-third of the world's biodiversity hotspots (Myers *et al.*, 2000) – regions that contain high levels of plant species richness and endemism yet are under threat from human activities – are located in temperate zones (Igea & Tanentzap, 2019), such as the five Mediterranean-type ecosystems (MTEs, i.e. California Floristic Region, Mediterranean Basin, Cape Floristic Province, Southwest Australia, Chilean Winter Rainfall-Valdivian Forests; Rundel *et al.*, 2016) and the Northern-Hemisphere mountain hotspots (e.g. Hengduan Mountains, Himalayas; Xing & Ree, 2017). A series of studies

\*These authors contributed equally to this work and share senior authorship.

has clarified patterns of high species richness and endemism in specific temperate areas, such as mountains, through uplift-driven diversification (Hughes, 2017; Zhang *et al.*, 2021). However, whether high diversification rates characterize temperate biodiversity hotspots more generally remains unclear due to the lack of a global analysis focused on temperate diversification. A global perspective is needed to understand whether temperate biodiversity is the result of similar drivers, such as climatic changes at global scales (e.g. global cooling and aridification since the Eocene–Oligocene boundary; Zachos *et al.*, 2001) and evolutionary processes (e.g. rapid speciation), or whether each region has a unique set of diversity drivers.

Current species diversity in temperate regions may be the outcome of three main evolutionary processes. First, *in situ* diversification rates – the balance between speciation and extinction within temperate regions – may have contributed to extant diversity. Indeed, many plant evolutionary radiations characterized by high diversification rates are thought to have occurred entirely in temperate biomes, such as the *Phyllica* (Rhamnaceae) and *Moraea* (Iridaceae) radiations in the Cape flora of southern Africa (Richardson *et al.*, 2001; Goldblatt *et al.*, 2002), and the *Dianthus* (Caryophyllaceae), *Tragopogon* (Asteraceae), and *Cistus* (Cistaceae) radiations in the Mediterranean Basin (Guzman *et al.*, 2009; Valente *et al.*, 2010; Bell *et al.*, 2012; Rundel *et al.*, 2016). Second, differences in historic rates of lineage dispersal can result in some temperate areas acting as ‘sources’, that is providing frequent dispersal of lineages emigrating to other regions where climatic conditions are suitable, and others as ‘sinks’, with high dispersal rates of lineages immigrating into the region, thereby increasing overall species richness. Immigration has been shown to play a significant role in the formation of regional biodiversity in the Hengduan Mountains and Himalayas (Xing & Ree, 2017; Ding *et al.*, 2020). Lastly, the time-for-speciation hypothesis (Stephens & Wiens, 2003) states that gradual diversification over time may lead to the build-up of species richness in a region, predicting that dispersal and diversification regimes do not differ among regions but instead regions that were colonized early harbor higher species richness than regions colonized later, either as a result of differences in biome or region age or differences in colonization opportunities. Time-for-speciation is often invoked to explain high diversity in the tropics, because tropical biomes are generally thought to be older than temperate ones, and may thus have accumulated diversity over longer periods of time (Mittelbach *et al.*, 2007; Pontarp *et al.*, 2019). Overall, contrasting mechanisms have been invoked to explain the distribution of biodiversity across individual temperate areas, but we lack global clarity on which processes are most important.

Macroevolutionary processes of lineage diversification, dispersal, and gradual diversity accumulation reflect a background of dynamic environmental and geological change. For example, although hot and humid rainforest biomes probably date back to the Cretaceous (*c.* 100 million years ago (Ma)) at middle paleolatitudes (Morley, 2000), climate cooling and aridification since the Eocene–Oligocene boundary (*c.* 34 Ma) has led to the global proliferation of temperate biomes (Zachos *et al.*, 2001; Palazzesi *et al.*, 2022). Expansion of temperate habitats is thought to have

provided ecological opportunities for lineages to colonize and diversify (Simpson, 1953; Donoghue, 2008; Stroud & Losos, 2016). Indeed, many temperate-adapted lineages evolved and diversified around and after the Oligocene, such as drought- and cold-adapted C<sub>4</sub> grasses (Poaceae), succulents (e.g. Aizoaceae and Cactaceae), and orchids (Orchidoideae), leading to the subsequent spread of grasslands and deserts (Arakaki *et al.*, 2011; Spriggs *et al.*, 2014; Palazzesi *et al.*, 2022; Thompson *et al.*, 2023a,b). In most of these cases, it is thought that lineages already possessed traits needed for colonizing a new region, and that the niche was largely conserved as lineages radiated after arrival (Wiens & Donoghue, 2004; Donoghue, 2008; Crisp *et al.*, 2009; Donoghue & Edwards, 2014). Thus, niche conservatism likely limits evolutionary transitions between biomes, especially between tropical and temperate biomes (Wiens & Donoghue, 2004; Crisp *et al.*, 2009), which greatly differ in terms of environmental challenges (Folk *et al.*, 2020). While rare, the gain of physiological adaptations to tolerate abiotic stress, such as freezing pressure, has been observed repeatedly across the angiosperm Tree of Life (Zanne *et al.*, 2018; Folk *et al.*, 2020). As a reflection of niche conservatism, it is thought that transitions from tropical to temperate biomes were facilitated by adaptations to seasonally dry tropical environments, because ancestral tropical lineages already possessed traits facilitating seasonal stressors such as drought complementary to the physiological traits needed for surviving freezes (Edwards *et al.*, 2017; Folk *et al.*, 2020). While such exaptations provided a means for tropical lineages to shift into temperate regions, these shifts were rare and it is more likely that lineage dispersals happened frequently between temperate regions, thereby contributing to the overall build-up of temperate biodiversity. Temperate biomes are also thought to differ in age across the globe, with old temperate biomes (e.g. sclerophyll biomes) tending to serve as a source for lineage dispersal to younger ones (e.g. arid, alpine, grassland) (Crisp *et al.*, 2009; Donoghue & Edwards, 2014). Thus, work to date suggests that any of the three potential diversity drivers (*in situ* diversification, dispersal, and time-for-speciation) may be responsible for centers of temperate diversity.

To understand the processes that underlie temperate centers of biodiversity, we examine historical eco-evolutionary dynamics through a suite of phylogenetic comparative methods with a focus on one angiosperm clade. We defined temperate biomes in terms of both geographic and Köppen–Geiger climatic definitions of tropics (Peel *et al.*, 2007), because different criteria may result in different inferences (Feeley & Stroud, 2018). The geographic definition identifies the region outside the range between 23.4°N and 23.4°S as temperate biomes, whereas the climatic definition identifies the region with year-round monthly mean temperatures of < 18°C as temperate biomes. We hypothesize (H1) that the colonization of temperate biomes happened independently and contemporaneously across lineages, due to global cooling and drying since the Oligocene, leading to parallel origins of temperate environments on different continents. Second, we hypothesize (H2) that global and regional species richness in temperate biomes are the result of high *in situ* diversification rates, rather than high immigration rates or early colonization times.

Specifically, we expect that temperate systems provided novel ecological opportunities or 'adaptive zones' (Simpson, 1953) for increased diversification rates with limited immigration from tropical regions and relatively recent and similar colonization times across areas. This scenario down-weights models assuming gradual diversity accumulation over time, since it explicitly suggests late origination and provides little time for temperate diversity to differentially increase among areas. Finally, we hypothesize (H3) that movement between temperate regions is relatively common; that is, there are strong source-sink dynamics that provide an engine for the unequal accumulation of lineages in today's centers of diversity.

To test these hypotheses, we focus on the buckthorn family Rhamnaceae (Rosales), a clade with a nearly cosmopolitan distribution of *c.* 1100 species within 63 genera (POWO, <http://plantsoftheworldonline.org/>). Rhamnaceae comprise predominantly woody shrubs with sclerophyllous leaves, exhibiting high diversity in fire-prone scrublands in temperate Mediterranean-type ecosystems, but also occurring in desert environments and temperate to tropical forests (Medan & Schirarend, 2004; Ladiges *et al.*, 2005; Onstein *et al.*, 2015, 2016). We reconstructed and dated the most comprehensive Rhamnaceae phylogeny to date, with extensive sampling of genera and species (574 species in 58 genera, or *c.* 52.2% and 92.0%, respectively) and genetic regions (89 low-copy nuclear loci). We then defined geographic- and climatic-based temperate biomes, and reconstructed the diversification history of Rhamnaceae across the temperate biome as a whole, within the most species-rich regions, and across local assemblages, in an effort to identify cross-scale macroevolutionary processes.

## Materials and Methods

### Plant sampling, sequencing, and data processing

We sampled 574 Rhamnaceae species (*c.* 52.2% of the 1100 recognized species according to POWO) from 58 genera (of the 63 genera according to POWO), with representatives of all 11 tribes and 9 of 10 genera unassigned to any tribe (Richardson *et al.*, 2000a,b; Hauenschild *et al.*, 2016). Three species of Elaeagnaceae and one species each of Barbeyaceae and Dirachmaeae (Rosales) were included as outgroups (Li *et al.*, 2021).

Leaf material was collected from the following herbaria: A, AD, BRI, CAS, F, KUN, MEL, MO, NY, OS, PERTH, TEX, and US as well as from the field (Supporting Information Dataset S1), and total DNA was extracted using a modified CTAB method following the protocol described in Folk *et al.* (2021). Target enrichment probes (Folk *et al.*, 2021; Fu *et al.*, 2022) were used to capture 100 low-copy nucleotide genes, and hybridization enrichment sequencing (Hyb-seq) was conducted by Rapid Genomics (Gainesville, FL, USA). Raw sequenced reads were cleaned and filtered as follows: Illumina adapter sequence artifacts were trimmed, low-quality reads were discarded, and low-quality read ends were trimmed using TRIMMOMATIC v.0.32 (Bolger *et al.*, 2014). Assembly of the processed nuclear reads was performed using HYBPIPER v.1.2 (Johnson

*et al.*, 2016), a reference-based assembler, using the 100 protein sequences from *Arabidopsis thaliana* used for probe design as the reference. Reads were mapped to each reference using BLASTX v.2.7.1 (Camacho *et al.*, 2009), each gene was assembled *de novo* using SPADes v.3.12.0 (Bankevich *et al.*, 2012), and coding sequences were extracted using EXONERATE v.2.4.0 (Slater & Birney, 2005). Each gene missing > 75% of the sampled species was excluded. As a result, 89 loci were kept for further analysis.

### Phylogenetic analyses and divergence time estimation

The sequences of each targeted gene region were initially aligned using MAFFT (Katoh & Standley, 2013) using default settings. To reduce errors in our alignments (i.e. gap-heavy and ambiguously aligned sites), we cleaned the original alignment of each gene using 'pxclsq' in PHYX (Brown *et al.*, 2017), removing alignment columns with < 30% occupancy. The cleaned alignments were concatenated into a supermatrix using the 'pxcat' function in PHYX. This supermatrix (Dataset S2) was then used to infer phylogenetic relationships in Rhamnaceae using the GTR-GAMMA model with 1000 bootstrap replicates in RAxML v.8.2.11 (Stamatakis, 2014). In addition, a coalescent species tree was inferred from the 89 best maximum likelihood (ML) single-gene trees, which were built in RAxML v.8.2.11 using the GTR-GAMMA model with 200 bootstraps (BS), using ASTRAL-III v.5.6.3 (Zhang *et al.*, 2018). Branches with < 10% BS in each gene tree were collapsed using Newick utilities (Junier & Zdobnov, 2010).

The concatenated supermatrix and the corresponding ML tree were used for dating analysis. We estimated divergence times using the penalized likelihood method implemented in TREEPL (Smith & O'Meara, 2012). Six fossils and a secondary calibration were used to calibrate node ages (more details in Methods S1). We used an optimal smoothing parameter determined by the 'random subsample and replicate' cross-validation method to accommodate rate heterogeneity. To assess uncertainty in age estimates, we estimated confidence intervals on inferred ages by dating all 100 ML bootstrap trees from the concatenated dataset (Maurin, 2020). Results from the dating of the bootstrapped trees were then summarized and visualized on the concatenated ML tree using TREEANNOTATOR v.2.6.3 (Bouckaert *et al.*, 2014).

### Global patterns of Rhamnaceae temperate biomes, species diversity, and biodiversity 'hotspots'

To illustrate the distribution and species richness of Rhamnaceae across temperate biomes, we collected occurrence data of all Rhamnaceae species from the global biodiversity information facility (GBIF, <https://www.gbif.org/>). The World Checklist of Vascular Plants (WCVP, <http://wcvp.science.kew.org/>) was used to standardize species with accepted names, and the infraspecific taxa and exotic and hybrid species were excluded. POWO was used to provide the native status for each species. These occurrence datasets were carefully assessed, and records that lacked geographic coordinates occurred in the oceans and were duplicates were removed by customized R scripts. Additionally, cultivation records were removed manually. Finally, a total of 291 041

unique distribution records from 1022 Rhamnaceae species, including 574 species used in the phylogenetic analysis, were used in subsequent steps (Dataset S3).

To identify the global temperate biomes, we initially divided the global map into the grid cells of  $1^\circ \times 1^\circ$ . Then, we used geographic and climatic definitions for the tropics (Peel *et al.*, 2007; Owens *et al.*, 2017) to classify grid cells as occurring in temperate or tropical (nontemperate) biomes. According to the geographic definition, we classified grid cells falling outside the range between  $23.4^\circ\text{N}$  and  $23.4^\circ\text{S}$  (the Tropics of Cancer and Capricorn) as temperate, while classified those within this range as tropical. According to the Köppen-Geiger climatic definition (Peel *et al.*, 2007), we classified grid cells with a year-round monthly mean temperature  $< 18^\circ\text{C}$  as temperate and classified those with a temperature  $\geq 18^\circ\text{C}$  as tropical (Dataset S4). In addition, we used these two definitions to classify each Rhamnaceae species as occurring in temperate and/or tropical biomes, while considering occurrence frequency, that is species with  $> 70\%$  of their occurrences in the temperate region were classified as temperate; species with  $> 70\%$  of their occurrences in the tropics were classified as tropical; otherwise, species were classified as both (temperate + tropical) (Dataset S5). We associated all grid cells and species occurrence points with average monthly annual mean temperature data using bio1 from WORLDCLIM (Fick & Hijmans, 2017).

To identify the global pattern of Rhamnaceae species richness, we matched the global filtered distribution dataset of 1022 species to the grid cells of  $1^\circ \times 1^\circ$  based on the presence/absence of species within each grid cell (Dataset S4). We then calculated the species richness of each grid cell using the R package PHYLOGEON (Daru *et al.*, 2020). We conducted an optimization analysis using the  $G_i^*$  local statistic (Getis & Ord, 1996) implemented in QGIS v.3.2 with the Hotspot Analysis plugin (Oxoli *et al.*, 2017) to identify regions particularly species-rich, hereafter Rhamnaceae ‘hotspots’. This method calculated the local spatial autocorrelation to cluster grid cells of high species richness. We identified each hotspot as a region consisting of adjacent grid cells with  $Z$  scores  $\geq 1.65$  (Suissa *et al.*, 2021), enforcing at least 30 grid cells per hotspot to ensure that each hotspot has a sufficient sample size and spatial extent. Once hotspots were identified, we defined nonhotspot regions as all remaining grid cells with at least one Rhamnaceae species (Dataset S4). Finally, we assessed whether the same hotspots were identified when we only included Rhamnaceae species that were sampled in the phylogenetic tree. Therefore, we calculated Spearman’s correlation between grid-based species richness when including all species distribution data ( $n = 1022$  species) to species richness when including only phylogenetically sampled species ( $n = 574$  species) (Spearman’s  $\rho = 0.93$  in our dataset).

### Environmental niche of temperate biomes and biodiversity hotspots

To characterize and compare the environmental conditions in temperate biomes and hotspots, we collected 35 environmental variables, including 19 bio-climatic variables at 2.5 m resolution

(<https://www.worldclim.org>), two topographical layers (<https://lta.cr.usgs.gov/GTOPO30>), eight soil layers (averaged in QGIS across layers at 5-, 15-, 30-, and 60-cm sampling depths; <https://soilgrids.org/>), and six land cover classes (<https://www.earthenv.org/landcover>). All environmental variables were extracted as mean values per  $1^\circ \times 1^\circ$  grid cells using the zonal statistics in the QGIS v.3.2 (QGIS Development Team, 2018). Mean values of the variables for each grid cell were used in the subsequent environmental niche analysis (Dataset S4).

To assess whether high Rhamnaceae species richness calculated from 1022 species was linked to environmental conditions typical for temperate biomes, and to assess whether hotspots shared such environmental space, we performed principal coordinate analyses (PCoA). All environmental variables (i.e. climate, topography, soil, and land cover) were log-transformed to improve homoscedasticity, and we scaled them between 0 and 1 to impose equal variable weight. PCoA was computed to describe the composition of environmental space of each hotspot region, using Euclidean dissimilarities calculated in the R packages VEGAN (Dixon, 2003) and APE (Paradis *et al.*, 2004). The volume of the convex hull composed of two independent axes (PCoA1 and PCoA2, collectively capturing 59.6% of the environmental variation) was then used to measure the overlap in climatic hypervolume space of temperate biomes and for each Rhamnaceae hotspot region.

### Inference of biogeographic history of biodiversity hotspots

To assess the independent and contemporaneous colonization of temperate regions (H1) and subsequent diversity accumulation through time (H2), we traced the biogeographic history of Rhamnaceae lineages across the temperate hotspots. Ancestral ranges were inferred by implementing a series of biogeographic models in the R package BIOGEOBEARS v.1.1.2 (Matzke, 2013). Outgroups were excluded from the time-calibrated phylogenetic tree. We used the corrected Akaike information criterion (AICc) to compare the fit of three biogeographical models: DEC, DIVALIKE, BAYAREALIKE, and versions of these three models that allowed for founder event speciation (+J) (Matzke, 2014), that is DEC+J, DIVALIKE+J, and BAYAREALIKE+J. We defined eight areas, following our identification of Rhamnaceae hotspot regions: California, Mexico–Central America, Mediterranean Basin, Southern China, South African Cape, Southwest Australia, Southeast Australia, and nonhotspot. Species were assigned to one or more biogeographic areas based on occurrence frequency within these regions, with presence only being assigned if species with  $> 10\%$  of its occurrences fell within a particular biogeographic area. The maximum number of areas was set to three, to reflect distributions of extant taxa.

We performed 100 biogeographical stochastic mappings (BSMs) (Dupin *et al.*, 2016) with the parameter rate estimates of the best-fitting model from the BioGeoBEARS analysis. The BSMs produced a probabilistic sample of the chronology of anagenetic and cladogenetic events, which allowed us to count and date anagenetic dispersals, extinctions, cladogenic range expansions (i.e. sympatry), and founder events. In addition, we binned

these events into 0.5-Ma periods and calculated the 95% confidence interval of the number of lineages occupying each region at each time step from 100 BSMs using the R package LTSTR (Skeels, 2019). Then, we extracted median values from the 95% confidence intervals to calculate the relative proportion of lineages in each hotspot and nonhotspot at each time bin.

### Diversification and dispersal rates of biomes and biodiversity hotspots

To assess whether high *in situ* diversification rates explained high Rhamnaceae species richness in temperate biomes and hotspots (H2) and whether the dispersal of lineages between temperate regions was relatively common (H3), we estimated speciation, extinction, and dispersal rates with the Geographic State Speciation and Extinction (GeoSSE) model (Goldberg *et al.*, 2011) implemented in the R package DIVERSITREE (FitzJohn, 2012). To this end, we used the classification of species as assigned above as ‘temperate’, ‘tropical’, or ‘both’. Furthermore, we also fitted GeoSSE models in which we classified species for each hotspot region (California, Mexico-Central America, Mediterranean Basin, Southern China, South African Cape, Southwest Australia, and Southeast Australia) against species occurring elsewhere, that is seven analyses in total. ‘Elsewhere’ therefore includes species occurring in all other recognized hotspots (except the specific hotspot of interest) as well as Rhamnaceae occurring in ‘nonhotspot’ regions. Each species was assigned to a hotspot based on its occurrence frequency (i.e. species with >90% of occurrences within a specific hotspot were assigned to that hotspot). Species with >90% of their occurrences outside any recognized hotspot were classified as occurring ‘Elsewhere’; finally, species were classified as widespread if they occurred both in specific hotspot and ‘Elsewhere’ (i.e. species with >10% and <90% of their occurrences within a specific hotspot). In addition, we ran another analysis in which we contrasted species in any hotspot region to species in nonhotspot areas.

All diversification analyses were conducted on the time-calibrated phylogenetic tree without outgroups. We compared the fit of eight models that allowed speciation, extinction, and dispersal rates to vary between temperate and tropical biomes or between lineages in hotspots vs ‘Elsewhere’ and selected the best-fitting model as assessed by a likelihood ratio test. The best-fit model was then used in a subsequent Bayesian MCMC run for 5000 generations (ESS > 200), using ML rate estimates as starting points and an exponential prior whose distribution was in relation to the overall diversification rate, estimated using the Kendall–Moran estimate for net diversification rate (Kendall, 1949; Moran, 1950). Because species in the Mediterranean Basin hotspot and the Southwest Australian hotspot consisted of <10% of the total species richness of Rhamnaceae, we were not able to infer rates for these hotspots individually due to sample size constraints (Davis *et al.*, 2013), but they were included in the analysis in which all hotspots were combined and compared with diversification and dispersal rates in nonhotspots.

### Phylogenetic assemblage structure of biodiversity hotspots

Another signature of high diversification rates can be captured by phylogenetic clustering – that is, species within a local assemblage are phylogenetically more closely related than expected by chance, suggesting *in situ* diversification from a common ancestor. We therefore calculated the net relatedness index (NRI) (Webb *et al.*, 2002) for each grid cell that contained more than one Rhamnaceae species ( $n = 3266$ ). NRI measures how mean phylogenetic distance between all species pairs in a grid cell deviates from a null model generated by shuffling taxa labels across the tips of the phylogeny. The calculation of NRI and associated 999 randomization tests was conducted with the R package PICANTE (Kembel *et al.*, 2010), and values were compared between assemblages in temperate and tropical biomes and hotspots.

### Sensitivity of macroevolutionary processes to hotspot definitions

To test whether diversification rates, dispersal rates, and colonization time inferences were robust to the size of hotspot delimitations from the  $G_i^*$  local statistic, we used a distance of 1 degree as a buffer distance around each hotspot (hereafter buffer hotspots), and repeated the BioGeoBEARS, BSMs, and GeoSSE, analyses with this new classification. All analyses above were carried out in R (R Core Team, 2022), unless mentioned otherwise.

## Results

### Phylogenetic analyses and divergence time estimation

After assembling and filtering, 89 low-copy nuclear genes were obtained for 574 Rhamnaceae species and five outgroup species. The concatenated data matrix was 93 936 bp in length. The three main Rhamnaceae groups, that is the rhamnoid group, the ziziphoid group, and the clade containing several Rhamnaceae taxa of few genera (*Bathiorhamnus*, *Doerpfeldia*, *Sarcomphalus*, and *Ziziphus*), were fully supported in the phylogeny (BS = 100%; LPP = 1) using both concatenation and coalescent methods (Figs 1a, S1, S2). The concatenated ML tree and coalescent ASTRAL tree were largely congruent, with most of the deeper nodes and branches resolved and strongly supported, except for a few nodes within the ziziphoid clade (Figs S1, S2). These showed conflicts and obtained relatively low support. Rhamnaceae were estimated to have originated at *c.* 113.54 Ma (113.33–113.60 Ma; 95% confidence interval) in the Cretaceous based on the concatenated ML tree, and details for the age estimates of clades are presented in Fig. S3.

### Global patterns of species diversity, temperate biomes, and biodiversity hotspots in Rhamnaceae

Based on the global species richness map (Fig. 2a), Rhamnaceae species diversity was markedly higher in temperate (mid-latitude) than in tropical (low-latitude) regions (Fig. 2b), resulting in a bimodal latitudinal diversity gradient. Rhamnaceae assemblages

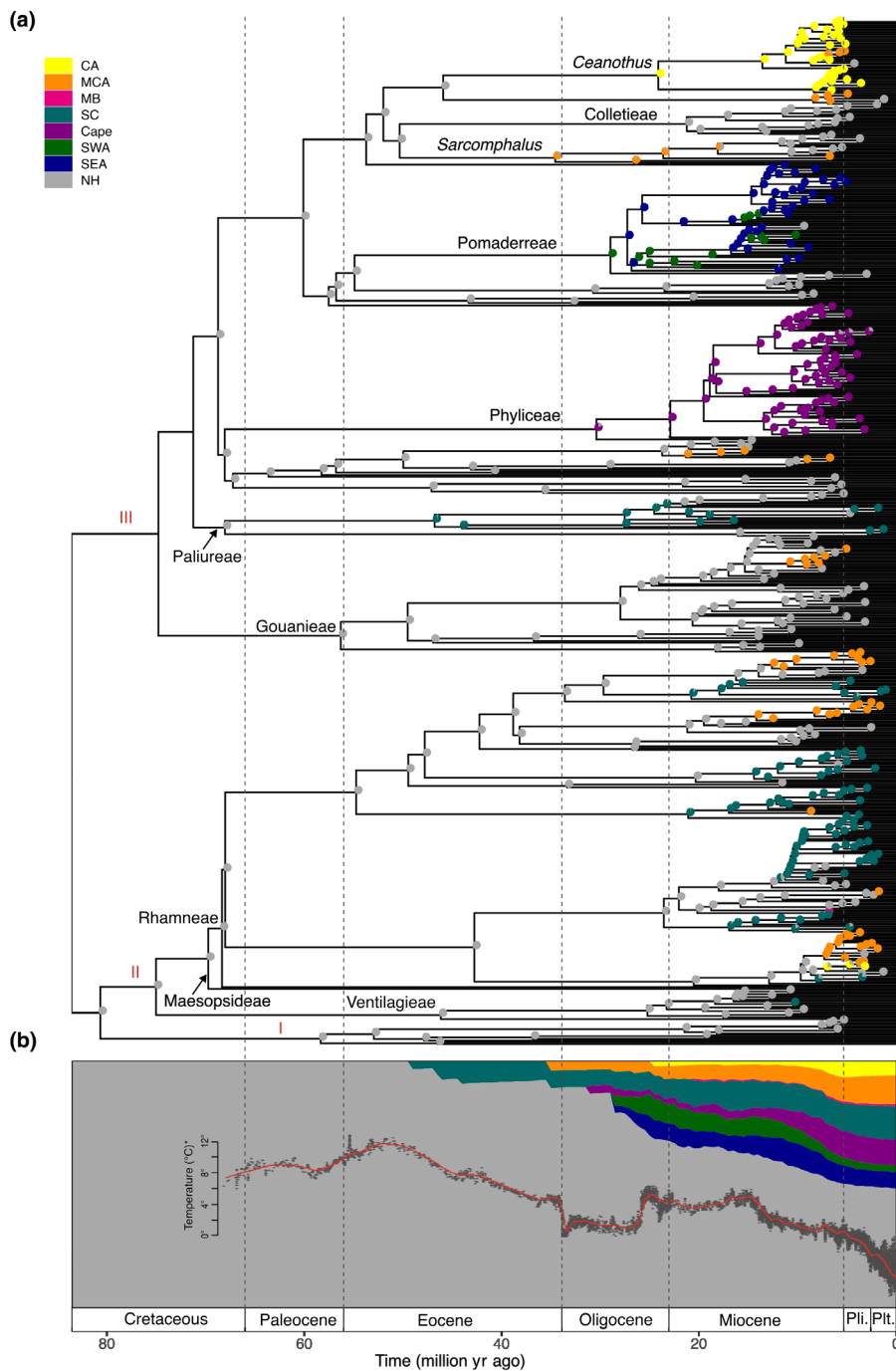


**Fig. 1** Ancestral range estimates and time for speciation of Rhamnaceae lineages in biodiversity hotspots. (a) Divergence times estimated using TREEPL based on the concatenated supermatrix of 89 low-copy loci, and the ancestral areas reconstructed by BioGeoBEARS using the BAYAREALIKE + J model. Pie charts at each node correspond to ancestral reconstructions and are color-coded for the area with the probability of each area. Only the probability > 50% of each hotspot in each node is colored. I, the group containing genera (*Bathiorhamnus*, *Doerpfeldia*, *Sarcomphalus*, and *Ziziphus*); II, the rhamnoid group; III, the ziziphoid group. CA, California; Cape, South African Cape; MB, Mediterranean Basin; MCA, Mexico-Central America; NH, nonhotspot; SC, Southern China; SEA, Southeast Australia; SWE, Southwest Australia. (b) Colonization and time for speciation of Rhamnaceae lineages in biodiversity hotspots. The relative proportion of lineages in each hotspot region through time, estimated from the biogeographical stochastic mappings (BSMs) analysis using a sliding window and median value from the 95% confidence interval of the number of lineages occupying each region at each time bin. The global temperature curve is taken from Zachos *et al.* (2001, reprinted with permission from AAAS) over the past 65 million years. Pli., Pliocene; Plt., Pleistocene.

and species were predominantly temperate based on geography (60.85% assemblages and 61.06% species) but not based on temperature (50.45% assemblages and 49.51% species; Datasets S4, S5). Some species were scored as belonging to both temperate and tropical areas (4.30% and 12.16% based on geographic and climatic definitions, separately), so tropical percentages were lower than temperate for both definitions. We identified seven distinct regions as 'hotspots', that is regions that comprise much higher species richness than nonhotspots ( $Z$  scores  $\geq 1.65$ ; Figs 2a, S4; Dataset S4): California ( $n = 60/48$  (number of occupied grid cells/species)), Mexico-Central America ( $n = 224/107$ ), Mediterranean

Basin ( $n = 57/10$ ), Southern China ( $n = 221/118$ ), South African Cape ( $n = 33/136$ ), Southwest Australia ( $n = 51/95$ ), and Southeast Australia ( $n = 126/116$ ). Grid cells outside the seven hotspots, defined as 'nonhotspots', were more numerous ( $n = 5254/553$ ).

#### Similarities in environmental features across temperate Rhamnaceae hotspots

We quantified the hypervolume of the environmental space as defined by PCoA1 (explaining 38.9% of the variance) and PCoA2 (20.7%) in temperate biomes and each hotspot (Fig. 3).

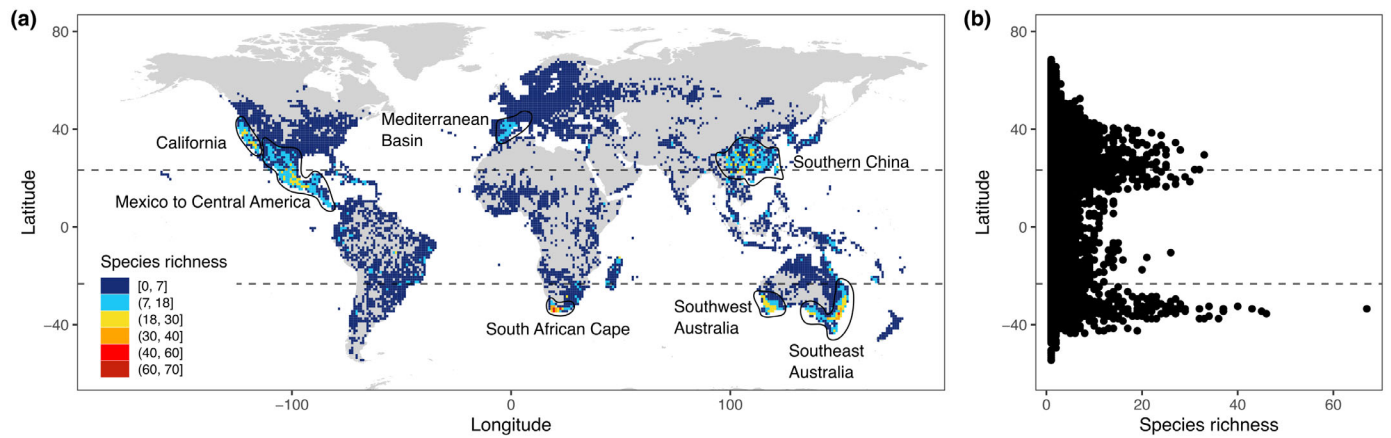


**Fig. 2** Global distribution of Rhamnaceae species richness across assemblages in the temperate realm. (a) Rhamnaceae species richness estimated from 291 041 unique distribution records of 1022 species. Colored squares indicate estimated species richness in grid cells of  $1^\circ \times 1^\circ$ . Regions containing hotspots of Rhamnaceae diversity outlined with solid lines. Dashed lines represent the Tropics of Cancer and Capricorn. (b) Species richness across latitude. Each point represents the species richness within a  $1^\circ \times 1^\circ$  grid cell plotted against the grid cell's latitudinal centroid.

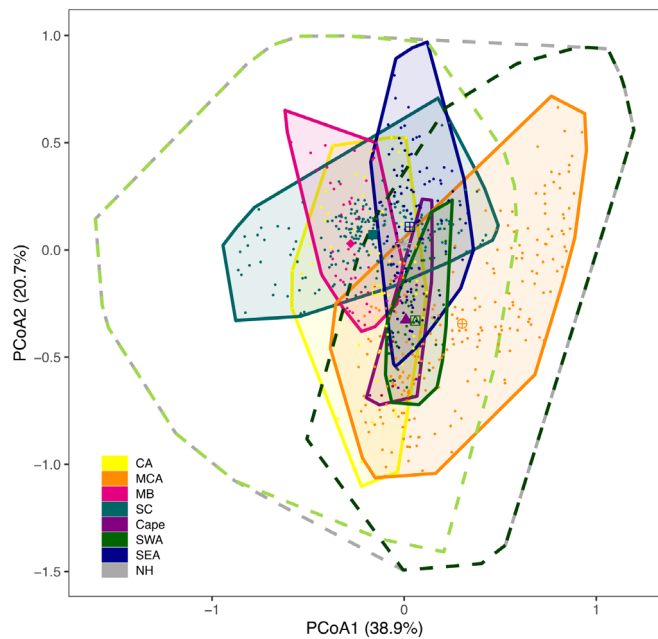


**Fig. 3** Occupancy of hypervolume environmental space in Rhamnaceae geographic-based temperate and tropical biomes and each diversification hotspot. Colored polygons are two-dimensional environmental hypervolumes based on 772 assemblages (grid cells) in seven hotspots using principal coordinates analysis (PCoA). The light green, dark green, and gray dashed polygons are the environmental hypervolumes of temperate and tropical biomes, as well as nonhotspot regions, respectively. Colored points represent grid cells. Colored shapes are hypervolume centroids. CA, California; Cape, South African Cape; MB, Mediterranean Basin; MCA, Mexico-Central America; NH, nonhotspot; SC, Southern China; SEA, Southeast Australia; SWE, Southwest Australia.

The PCoA showed that environmental space of all hotspots was nested within the temperate biome environmental space according to both geographic and climatic definitions (Figs 3, S5a), with the exception of parts of Mexico-Central America. The

environmental space in Mexico-Central America was more diverse, spanning temperate to tropical biomes (Figs 2, 3, S4, S5). Furthermore, the PCoA showed substantial overlap (on average 14.8–56.4% per hotspot; Table S1) among the seven hotspots in environmental hypervolume space. A biplot showed that temperature variables (e.g. isothermality and annual mean temperature) along the PCoA1 axis and soil variables (e.g. soil organic carbon and soil pH) along the PCoA2 axis were the most important predictors of the environmental hypervolume (Fig. S5b). The biplot also showed tropical climatic features (right side of the biplot) in Mexico-Central America, relatively nutrient-rich soils in the Southeast Australia hotspot (top side of the biplot), and colder temperatures in the Southern China hotspot (left side of the biplot), that distinguish environments in these hotspots from the other hotspots.

### Historical biogeography of hotspots

The BioGeoBEARS and BSMs analyses were used to infer the colonization time of each hotspot relevant to assess H1, and to evaluate the time-for-speciation within each region relevant for testing H2. The BAYAREALIKE + J model was selected in the ancestral biogeographic reconstruction of Rhamnaceae hotspots based on the AICc (Table S2; Fig. S6). By comparing the relative accumulation of lineages through time in each hotspot (Fig. 1b), we detected the earliest colonization of the temperate region at *c.* 49.0 Ma (46.5–83.5 Ma; 95% confidence interval of age of lineages occupying each region from 100 BSMs), that is with the colonization of Southern China during the Eocene. Subsequently, lineages independently colonized Mexico-Central America at *c.* 35 Ma (29.5–83.5 Ma), the South African Cape at *c.* 31.0 Ma (23.0–83.5 Ma), Southwest Australia at *c.* 28.5 Ma (28.5–83.5 Ma), Southeast Australia at *c.* 28.5 Ma (27.0–57 Ma), and California at *c.* 24.5 Ma (24.5–62.0 Ma). Thus, Rhamnaceae achieved their modern distribution through a series of largely contemporaneous dispersals during the Oligocene, consistent

with H1. Lineages colonized the Mediterranean Basin somewhat later during the early Miocene, *c.* 20.5 Ma (7.0–83.5 Ma). We found that the proportion of Rhamnaceae lineage diversity in the hotspot regions compared with elsewhere continued to increase rapidly and in parallel across hotspots from the Miocene onward. The BAYAREALIKE model was selected in the biogeographic analysis of buffer hotspots (Table S2), but ancestral biogeographic reconstruction, colonization times, and lineage accumulation curves in buffer hotspots were similar overall to those in the main hotspot analysis (Figs S6–S8).

### Macroevolutionary rates of diversity in hotspots

The GeoSSE analyses were used to infer *in situ* diversification and dispersal rates linked to H2, and to evaluate source-sink dynamics (i.e. dispersal rate asymmetries) relevant for testing H3. The best-fitting GeoSSE models indicated distinct diversification and/or dispersal rates for temperate vs tropical biomes, and for each hotspot vs ‘Elsewhere’, based on likelihood ratio tests (Table S3). Lineages in temperate biomes showed higher speciation and net diversification rates than lineages in tropical biomes, a result that was robust to geographic (Fig. 4a,c) and climatic (Fig. S9a,c) definitions of temperate biomes. Furthermore,

lineages occurring in hotspots showed higher net diversification rates than lineages occurring ‘Elsewhere’, except Southern China, thus mostly consistent with H2, but speciation and extinction rates differed among the five hotspots (Fig. 4e–g). Specifically, California, South African Cape, and Southeast Australia showed higher speciation rates, resulting in higher net diversification rates for lineages in these hotspots than lineages in Mexico-Central America and Southern China. For Mexico-Central America, the lowest speciation rates resulted in relatively low net diversification rates. For Southern China, the relatively low speciation rates and the highest extinction rates resulted in the lowest net diversification rates across hotspots, similar to diversification rates in non-hotspots. Rates of speciation, extinction, and net diversification in buffer hotspots were qualitatively similar to those in hotspots (Figs 4e–g, S9d–f).

GeoSSE results showed equal migration and immigration (i.e. dispersal) rates between temperate and tropical regions according to the geographical definition (Fig. 5). Furthermore, dispersal rates from hotspots to ‘Elsewhere’ were significantly higher than vice versa in all five hotspots (Fig. 5), consistent with H3. Among hotspots, we found that dispersal rates out of Mexico-Central America and Southern China were comparatively high, while dispersal rates out of the South African Cape and Southeast Australia

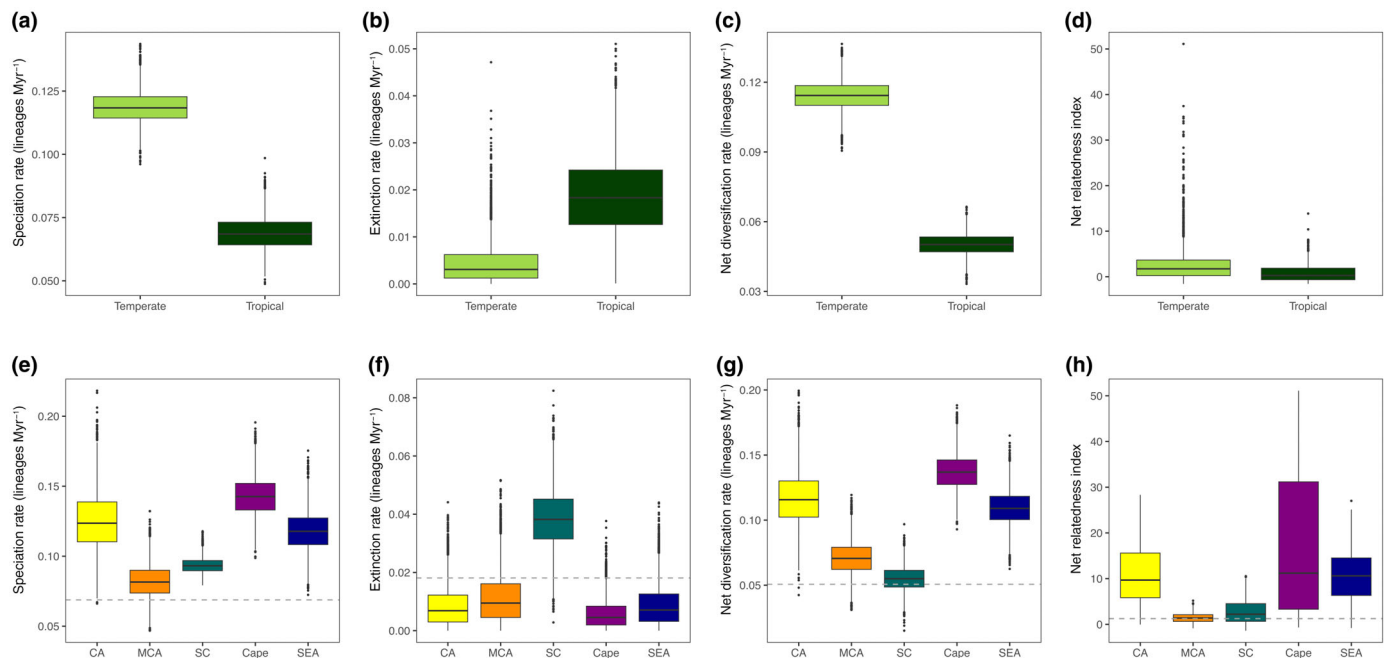
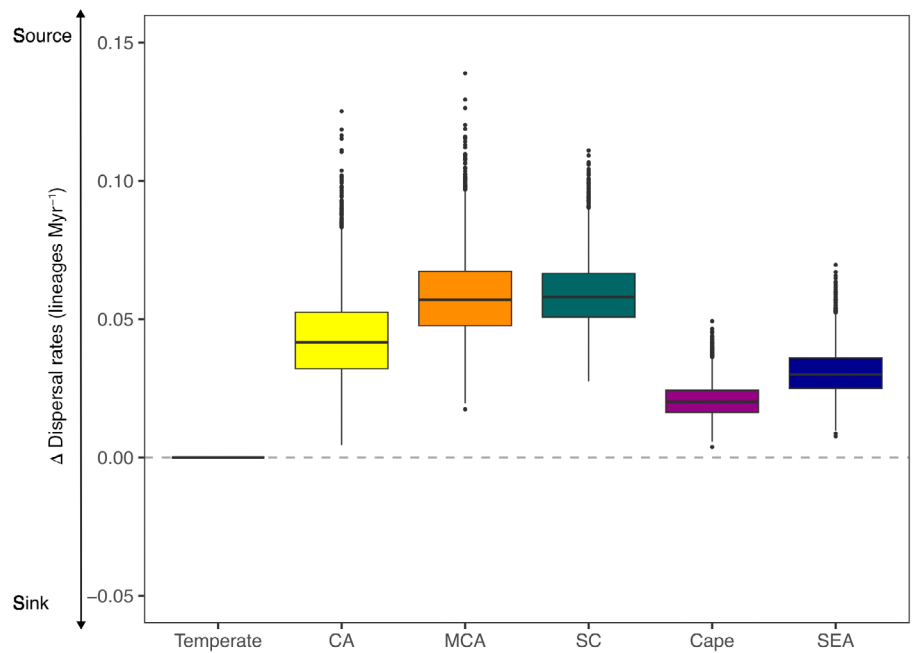


**Fig. 4** Diversification rates and net relatedness index (NRI) across geographic-based temperate and tropical biomes and each diversification hotspot in Rhamnaceae. Estimated parameter distributions in temperate vs tropical biomes as well as of Rhamnaceae lineages evolving in one hotspot vs ‘Elsewhere’ (all other hotspots plus nonhotspots). The Mediterranean Basin and Southwest Australia were excluded because sampling of species in these two hotspots was < 10% compared with ‘Elsewhere’. Boxplots show (a) speciation rates (lineages million years (Myr)<sup>-1</sup>), (b) extinction rates (lineages Myr<sup>-1</sup>), (c) net diversification rates (lineages Myr<sup>-1</sup>), and (d) NRI of temperate and tropical biomes; (e) speciation rates (lineages Myr<sup>-1</sup>), (f) extinction rates (lineages Myr<sup>-1</sup>), (g) net diversification rates (lineages Myr<sup>-1</sup>), and (h) NRI of the five hotspots. Boxes in figures (a–c, e–g) are colored by region and represent parameter distributions from the Bayesian MCMC using the best-fitting GeoSSE model on the time-calibrated Rhamnaceae phylogenetic tree. The upper boundary of each box represents the third quartile (Q3), the lower boundary represents the first quartile (Q1), the horizontal line inside the box represents the median (Q2), and the extending lines (whiskers) display the maximum and minimum values, excluding outliers identified by filled circles. Dashed lines shown in figures (e–h) are averaged parameter values of nonhotspot lineages. CA, California; Cape, South African Cape; MCA, Mexico-Central America; SC, Southern China; SEA, Southeast Australia.

**Fig. 5** Source and sink dynamics of Rhamnaceae in geographic-based temperate biomes and each diversification hotspot. Boxes are colored by region and represent parameter distributions (dispersal rates out of a region minus dispersal rates into that region) from the Bayesian MCMC from the best-fitting GeoSSE model on the time-calibrated Rhamnaceae phylogenetic tree. The upper boundary of each box represents the third quartile (Q3), the lower boundary represents the first quartile (Q1), the horizontal line inside the box represents the median (Q2), and the extending lines (whiskers) display the maximum and minimum values, excluding outliers identified by filled circles. Above the dashed line represents the source, and below represents the sink. CA, California; Cape, South African Cape; MCA, Mexico-Central America; SC, Southern China; SEA, Southeast Australia.



hotspots were relatively low. Rates of dispersal in buffer hotspots were qualitatively similar to those in hotspots (Fig. S10).

Geographic and climatic definitions differed in inferences of extinction and dispersal rates between temperate and tropical biomes. Specifically, we inferred lower extinction rates in geographically temperate areas but equal extinction rates in climatically temperate areas (Figs 4b, S9b). Furthermore, climatically temperate areas showed higher dispersal rates to tropical areas than the reverse (Fig. S10), whereas dispersal rates were equal in geographically temperate areas (Fig. 5). Nevertheless, both geographical and climatic definitions consistently illustrated higher speciation and correspondingly higher net diversification rates in temperate biomes compared with tropical biomes, which explained high species richness. Therefore, we presented results based on the geographical definition in the main text, but provide results from the climatic definition in Figs S9 and S10. In addition, we plotted ancestral state estimates and per-state probabilities of Rhamnaceae biomes according to both the geographical and the climatic definitions from the best-fitting GeoSSE models (Figs S11, S12).

### Phylogenetic clustering of lineages in hotspots

Net relatedness index showed significant phylogenetic clustering in temperate compared with tropical biomes, as well as within assemblages in California, South African Cape, and Southeast Australia (Figs 4d,g, S13), suggesting that these assemblages are composed of closely related species, thus consistent with high, primarily *in situ* diversification rates in these hotspots (supporting H2, Fig. 4). By contrast, the NRI comparison among the seven hotspots indicated that both Mexico-Central America and Southern China had an overall random/overdispersed structure with relatively low NRI compared with those of the other hotspots,

suggesting that assemblages are instead composed of distantly related species that may reflect multiple dispersal events into and/or out of these regions.

### Discussion

We dissected relationships between environment, diversification, and dispersal to understand high biodiversity in temperate biomes across global, regional, and local scales, using Rhamnaceae as a model system. We identified temperate biomes at the global level and seven hotspots particularly high in Rhamnaceae species richness: California, Mexico-Central America, Mediterranean Basin, Southern China, Cape, Southwest Australia, and Southeast Australia (Figs 2a, S4). Most hotspots are located within temperate regions according to the geographic and climatic definitions of temperate biomes, except for Mexico-Central America, which spans temperate to tropical biomes. With Southern China as an exception, our results overall point to high *in situ* diversification rates (Figs 4, S9), rather than high immigration rates or accumulative time (Figs 1b, 5, S9, S10) as the primary process behind the high diversity of Rhamnaceae in temperate biomes.

We show that all Rhamnaceae hotspots overlap in current environmental space, particularly in the climatic facets most important for defining the unique stressors of temperate – and especially Mediterranean – ecosystems (Figs 3, S5). Notably, California, the Mediterranean Basin, South African Cape, and Southwest Australia all share a Mediterranean climate with dry, hot summers, cooler, wet winters, and fire-prone and woody shrubland vegetation (Donoghue & Edwards, 2014; Rundel *et al.*, 2016). This overlap in environment among Rhamnaceae hotspots, which comprise phylogenetically disparate species clusters and independent colonizations from tropical ancestors

during the Oligocene (Fig. 1b), suggests an important role of niche conservatism or evolutionary predisposition in the assembly of Rhamnaceae across the temperate biomes (Crisp *et al.*, 2009; Ackerly & Onstein, 2018). In addition, the similarity in environmental space highlights a possible role of ecological sorting (Ackerly, 2004). Indeed, before the emergence of Mediterranean climates, similar environments in the Mediterranean regions may have filtered for lineages possessing functional traits (e.g. small, evergreen, and sclerophyllous leaves) that facilitated survival on old, stable, infertile soils (Hopper, 2009; Onstein *et al.*, 2016; Ackerly & Onstein, 2018).

Rhamnaceae colonizations of several geographically separated temperate regions show a striking similarity in timing (i.e. 35–24.5 Ma), but lineage diversity increases in these biomes later, particularly so from 23 Ma onward (Figs 1b, S8). We argue that diversity within the Mediterranean temperate hotspots has resulted from a set of *in situ* – possibly nested – radiations, where a combination of global climate change and preadapted traits (e.g. sclerophyllous leaves) facilitated parallel and rapid diversification across seasonal and xeric climatic regions (Onstein *et al.*, 2016; Rundel *et al.*, 2016). This is consistent with H1, namely that the global expansion of temperate biomes from the Oligocene onward (34 Ma) due to strong climate cooling events and drying, provided ecological opportunities for temperate biodiversity to originate and expand. Similar patterns of increased diversification coinciding with the onset of colder and drier climates in the Miocene have been found in some angiosperm lineages, such as Poaceae, Asteraceae, Saxifragales, rosids, and orchids (Folk *et al.*, 2019; Soltis *et al.*, 2019; Sun *et al.*, 2020; Palazzesi *et al.*, 2022; Thompson *et al.*, 2023a).

Lineages in California, South African Cape, and Southeast Australia showed high speciation and low extinction rates and strong phylogenetic clustering of assemblages (Fig. 4d–g). Our results are consistent with the many evolutionary radiations characterized in Rhamnaceae in previous work, such as *Ceanothus* (c. 60 species) in Californian chaparral (Burge *et al.*, 2011), Phyllaceae (c. 150 species) in South African Cape fynbos (Linder, 2003), and Pomaderreae (c. 240 species) in Australian shrublands (Kellermann, 2020; Nge *et al.*, 2021). Furthermore, Rhamnaceae share this signature of high diversification with other lineages in these regions, such as *Arctostaphylos* (Ericaceae) in California (Stebbins & Major, 1965), *Moraea* (Iridaceae) in the South African Cape (Goldblatt *et al.*, 2002), and *Acacia* (Caesalpinioideae) in Australia (Renner *et al.*, 2020). Although Mexico-Central America showed phylogenetic overdispersion, and it harbors distinct Rhamnaceae lineages (*Ceanothus*, *Colubrina*, *Sarcomphalus*, and Rhamneae), these lineages showed overall high net diversification rates compared with Rhamnaceae lineages evolving ‘Elsewhere’ (Fig. 4d–g). It is likely that the phylogenetic overdispersion here may be related to high mixed endemism and high diversity of Mexico-Central America, as this region is at a crossroads between temperate and tropical regions and also has highly heterogeneous environments because of its topographic complexity – a unique combination (Sosa *et al.*, 2018). Therefore, our results are consistent with H2, that is that high *in situ* diversification rates explain high species richness.

The exception to the high *in situ* diversification of Rhamnaceae in hotspots is Southern China. Here, lineages showed relatively low speciation rates and high extinction rates, resulting in much lower net diversification rates than lineages in any of the other hotspots, similar to rates in nonhotspot areas (Fig. 4d–g). Furthermore, assemblages in Southern China showed phylogenetic overdispersion (Fig. 4g), comprising distinct Rhamnaceae lineages (e.g. *Rhamnus*, *Berberia*, *Rhamnella*, and *Ziziphus*), and the region was colonized much earlier than the other regions (Figs 1b, S8). High species richness in Southern China may therefore be explained by the time-for-speciation hypothesis, with gradual accumulation of species diversity since the Eocene (Yan *et al.*, 2018). Even though NRI is similar between Southern China and Mexico-Central America compared with the other three hotspots (Fig. 4h), it has potentially resulted from different evolutionary processes (Fig. 4e,f) – thus, different extinction rates can create similar assemblage NRI patterns. Our results emphasize that we cannot fully understand past evolutionary processes by simply looking at NRI patterns of assemblages today. It has been suggested that extinction over time may be the reason for phylogenetic overdispersion in Southern China (Zhang *et al.*, 2022). Indeed, Southern China is a center of paleo- and mixed paleo/neo-endemism of woody plants (Wang *et al.*, 2022) and acts as refugium (i.e. paleo-endemism) for rare Chinese angiosperms, characterized by magnoliids and other ancient angiosperm lineages that survived extinction events and persist in a much narrower area than previously or places of more recent diversification (i.e. neo-endemism) (Lu *et al.*, 2018; Wang *et al.*, 2022; Zhang *et al.*, 2022). Orogenic movements, annual temperature, and annual precipitation may have experienced little change in mountainous areas of this region since the Cretaceous (Lu *et al.*, 2018), and long-term climate stability may have provided the opportunity for some but not all lineages to persist in this refugial landscape. Thus, our results for Rhamnaceae provide macroevolutionary evidence that is consistent with Southern China, but not other hotspots, namely that long-term stability may facilitate the gradual accumulation of diversity over geological time.

Our GeoSSE analysis showed that dispersal rates out of temperate biomes were equal or higher than out of tropical biomes overall, and dispersal rates into hotspots were significantly lower than dispersal rates out of hotspots (Figs 5, S10; also see Onstein *et al.*, 2015), suggesting that while hotspots differed in dispersal rates, it is unlikely that high immigration rates have influenced the globally high Rhamnaceae species richness in temperate biomes, which is consistent with H2. In addition, our results suggest that Rhamnaceae temperate hotspots may have acted as sources for recruitment of species in neighboring areas, that is primarily nonhotspot temperate regions (e.g. *Ceanothus* dispersal to regions outside the Mexico-Central America hotspot, *Phyllica* dispersal to regions outside the South African Cape hotspot), making the hotspots ‘source’ rather than ‘sink’ regions. The creation of such a source may be linked to the high *in situ* diversification rates in these regions, resulting in high numbers of lineages and species. Our results suggest that these dispersals may have been to both temperate and tropical biomes (Figs 5, S10–S12). Thus, reversals to more tropical systems (e.g. seasonally dry

tropical biome) from temperate regions are not uncommon in Rhamnaceae, probably because the temperate biomes they dominate are characterized by (seasonal) drought, rather than frost, which may be a less challenging transition to overcome physiologically (Figs S11, S12). Furthermore, our results suggest that Rhamnaceae lineages generally retained ancestral temperate niche preferences and were more often subject to dispersal into montane tropical biomes (i.e. climatically temperate biomes in the geographical tropics) (Owens *et al.*, 2017). Overall, our results do not point to dispersal rate asymmetries as a major explanation of temperate diversity, but they do suggest that movement between temperate regions is relatively common and reflects source–sink dynamics primarily between temperate regions, and thus consistent with H3.

Furthermore, we found that dispersal rates out of the Mexico-Central America and Southern China hotspots were higher compared with dispersal rates from any of the other hotspots (Figs 5, S10). These two hotspot regions cover a wide geographical distribution with high environmental heterogeneity (Figs 2, 3, S5a), the relatively higher proportion of unique climatic hypervolumes compared with other hotspots, thus possibly providing more opportunities for exchange of lineages with subjacent regions around these two hotspots. Moreover, Mexico-Central America forms a transition zone between the Nearctic and Neotropical biotas, and > 50% of Mexico is arid or semi-arid, which may have favored the dispersal of tropical lineages that were pre-adapted to survive under extreme seasonal and arid climates (Pennington & Lavin, 2016; Sosa *et al.*, 2018). However, the MTEs are heterogeneous in environment as well, characterized by the seasonal climate (i.e. extreme summer drought almost comparable to dry tropics as well as warm, wet winters comparable to mild temperate summer), in combination with differences in fire, topography, and soils, such as uplift, old bedrock and variation in soil types depending on the region, which could facilitate reproductive isolation and allopatric speciation (Onstein *et al.*, 2016; Rundel *et al.*, 2016; Ackerly & Onstein, 2018). This suggests that the availability of diverse, heterogeneous environments may also have contributed to the evolution of Rhamnaceae species richness, and these differences may also explain differences in ‘source’ and ‘sink’ dynamics between the regions (Fig. 5).

Finally, it is noted that many of these Rhamnaceae temperate hotspots are relatively young (e.g. MTEs) compared with the much earlier (Oligocene) colonization of these regions by Rhamnaceae (Onstein *et al.*, 2015), and diversification rates may have only shifted when climates changed (e.g. after the onset of the typical cool and dry MTE climate). However, the GeoSSE models we used here were not able to detect such time-dependent shifts in diversification rates within regions. Furthermore, model inferences may be biased by uncertainties in phylogenetic dating and disentangling speciation and extinction rates from phylogenies that include extant species only (Louca & Pennell, 2020). Information from, for example, paleoclimate data and fossils could improve historical model-based inferences and our understanding of temporal changes in macroevolutionary processes and their drivers.

In conclusion, our study offers an integrative approach to elucidate why certain temperate biomes, such as Mediterranean-type ecosystems, harbor high species diversity. We identify rapid *in*

*situ* diversification rates in response to the onset and expansion of temperate biomes in the Oligocene as the best explanation; this history left a consistent signature on Rhamnaceae species composition across spatial scales, both within the temperate biomes as a whole and in regional species-rich hotspots. Although we identified a consistent global pattern, we also detected region-specific histories, with some areas illustrating higher historical connectivity through lineage dispersals to other temperate and tropical systems (e.g. Southern China, Mexico-Central America) and others indicative of evolution *in situ*, reflecting their spatial isolation from other hotspots (e.g. South African Cape). Finally, our delineated species-rich regions broadly overlap with established biodiversity hotspots (Myers *et al.*, 2000; CEPF, 2016) except for Southern China, which was mostly unique to Rhamnaceae. However, Southern China features exceptional plant endemism across diverse lineages, which appears to have arisen from differing mechanisms and is under increasing human threat (López-Pujol *et al.*, 2011; Wang *et al.*, 2022). Overall, our study provides a large and well-supported case study of global diversity in temperate regions. Rhamnaceae are an excellent model system, with high diversity in multiple temperate hotspots, particularly within MTEs. More studies of widely distributed groups that exhibit diversity in temperate regions, such as Rosaceae, Iridaceae, and Fagales, can further test generalities about the processes underlying plant diversity in temperate biomes (e.g. Davies *et al.*, 2005; Xing *et al.*, 2014; Sun *et al.*, 2020).

## Acknowledgements

This research was supported by the National Natural Science Foundation of China, Key International (regional) Cooperative Research Project (no. 31720103903), the Strategic Priority Research Program of Chinese Academy of Sciences (no. XDB31000000), the Science and Technology Basic Resources Investigation Program of China (no. 2019FY100900), the National Natural Science Foundation of China (no. 31270274), the Yunling International High-end Experts Program of Yunnan Province, China (no. YNQR-GDWG-2017-002 and no. YNQR-GDWG-2018-012), the China Scholarship Council (202004910775), the CAS President's International Fellowship Initiative (no. 2020PB0009), the China Postdoctoral Science Foundation (CPSF), the International Postdoctoral Exchange Program, the CAS Special Research Assistant Project, a German Research Foundation grant to iDiv (DFG FZT 118, 202548816, acknowledged by REO), the Australian Biological Resources Study (grant no. RG18-25 to JK), and the US Department of Energy (grant no. DE-SC0018247 to PSS, RPG, and DES). We are grateful to the following institutions for providing specimens or silica-dried materials: Harvard University Herbaria (A); State Herbarium of South Australia (AD); Queensland Herbarium (BRI); the herbarium of the California Academy of Sciences (CAS); the Field Museum Herbarium (F); the herbarium of Kunming Institute of Botany, Chinese Academy of Sciences (KUN); the Germplasm Bank of Wild Species and Molecular Biology Experiment Center, Kunming Institute of Botany, Chinese Academy of Sciences; National Herbarium of Victoria

(MEL); the Missouri Botanical Garden Herbarium (MO); the New York Botanical Garden Herbarium (NY); the Ohio State University Herbarium (OS); Western Australian Herbarium (PERTH); the University of Texas Herbarium (TEX); and the United States National Herbarium (US). We are also grateful to Jiajin Wu for help with sampling and DNA extraction; to Ruijiang Wang for silica-dried materials of *Fenghwaia gardeniicarpa*; to Wubin Xu, Yahuang Luo, Tobias Nicolas Rojas, Friederike J.R. Wölke, Orlando Schwery, Lin Bai, Guangfu Zhu for their discussion and necessary assistance; and to the iFlora High Performance Computing Center of Germplasm Bank of Wild Species (iFlora HPC Center of GBOWS, KIB, CAS) for computing. Open Access funding enabled and organized by Projekt DEAL.

## Competing interests

None declared.

## Author contributions

T-SY, REO and QT designed the study. T-SY, QT, RAF, HRK and GWS collected and prepared samples for sequencing with contributions from JK, FJN and S-YL. QT performed data analysis with advice from REO. QT, REO and T-SY wrote the manuscript with contributions from RAF, RPG, PSS, DES, JK, DM and FJN. REO and T-SY contributed equally to this work and share senior authorship.

## ORCID

Ryan A. Folk  <https://orcid.org/0000-0002-5333-9273>  
 Robert P. Guralnick  <https://orcid.org/0000-0001-6682-1504>  
 Jürgen Kellermann  <https://orcid.org/0000-0001-9124-9802>  
 Shui-Yin Liu  <https://orcid.org/0000-0002-8674-7097>  
 Francis J. Nge  <https://orcid.org/0000-0002-0361-8709>  
 Renske E. Onstein  <https://orcid.org/0000-0002-2295-3510>  
 Douglas E. Soltis  <https://orcid.org/0000-0001-8638-4137>  
 Pamela S. Soltis  <https://orcid.org/0000-0001-9310-8659>  
 Gregory W. Stull  <https://orcid.org/0000-0002-2733-4823>  
 Qin Tian  <https://orcid.org/0000-0002-7939-5329>  
 Ting-Shuang Yi  <https://orcid.org/0000-0001-7093-9564>

## Data availability

The concatenated alignment supermatrix, occurrence, and climate data used in this study will be available in our [Supporting Information](#). Raw sequence data are available at the NCBI Sequence Read Archive (BioProject: [PRJNA1047935](#)). The aligned DNA sequences are available on Dryad Digital Repository: <https://datadryad.org/stash/dataset/doi:10.5061/dryad.gxd2547sq>.

## References

Ackerly DD. 2004. Adaptation, niche conservatism, and convergence: comparative studies of leaf evolution in the California chaparral. *The American Naturalist* **163**: 654–671.

- Ackerly DD, Onstein RE. 2018. Case study 2: assembly of Mediterranean-type floras: convergence, exaptation and evolutionary predisposition. In: Esler KJ, Jacobsen AL, Pratt RB, eds. *The biology of Mediterranean-type ecosystems*. Oxford, UK: Oxford University Press, 27–34.
- Arakaki M, Christin PA, Nyffeler R, Lendel A, Eggli U, Ogburn RM, Spriggs E, Moore MJ, Edwards EJ. 2011. Contemporaneous and recent radiations of the world's major succulent plant lineages. *Proceedings of the National Academy of Sciences, USA* **108**: 8379–8384.
- Bankevich A, Nurk S, Antipov D, Gurevich AA, Dvorkin M, Kulikov AS, Lesin VM, Nikolenko SI, Pham S, Pribelski AD *et al.* 2012. SPADes: a new genome assembly algorithm and its applications to single-cell sequencing. *Journal of Computational Biology* **19**: 455–477.
- Bell CD, Mavrodiev EV, Soltis PS, Calaminus AK, Albach DC, Cellinese N, Garcia-Jacas N, Soltis DE. 2012. Rapid diversification of *Tragopogon* and ecological associates in Eurasia. *Journal of Evolutionary Biology* **25**: 2470–2480.
- Bolger AM, Lohse M, Usadel B. 2014. TRIMMOMATIC: a flexible trimmer for Illumina sequence data. *Bioinformatics* **30**: 2114–2120.
- Bouckaert R, Heled J, Kuhnert D, Vaughan T, Wu CH, Xie D, Suchard MA, Rambaut A, Drummond AJ. 2014. BEAST 2: a software platform for Bayesian evolutionary analysis. *PLoS Computational Biology* **10**: e1003537.
- Brown JW, Walker JF, Smith SA. 2017. PHYX: phylogenetic tools for unix. *Bioinformatics* **33**: 1886–1888.
- Burge DO, Erwin DM, Islam MB, Kellermann J, Kembel SW, Wilken DH, Manos PS. 2011. Diversification of *Ceanothus* (Rhamnaceae) in the California Floristic Province. *International Journal of Plant Sciences* **172**: 1137–1164.
- Camacho C, Coulouris G, Avagyan V, Ma N, Papadopoulos J, Bealer K, Madden TL. 2009. BLAST+: architecture and applications. *BMC Bioinformatics* **10**: 1–9.
- CEPF. 2016. *Announcing the world's 36th biodiversity hotspot: the North American coastal plain*. [WWW document] URL <https://www.cepf.net/our-work/biodiversity-hotspots/hotspots-defined> [accessed 1 September 2022].
- Crisp MD, Arroyo MT, Cook LG, Gandolfo MA, Jordan GJ, McGlone MS, Weston PH, Westoby M, Wilf P, Linder HP. 2009. Phylogenetic biome conservatism on a global scale. *Nature* **458**: 754–756.
- Daru BH, Karunarathne P, Schliep K, Silvestro D. 2020. PHYLOREGION: R package for biogeographical regionalization and macroecology. *Methods in Ecology and Evolution* **11**: 1483–1491.
- Davies TJ, Savolainen V, Chase MW, Goldblatt P, Barraclough TG. 2005. Environment, area, and diversification in the species-rich flowering plant family Iridaceae. *The American Naturalist* **166**: 418–425.
- Davis MP, Midford PE, Maddison W. 2013. Exploring power and parameter estimation of the BiSSE method for analyzing species diversification. *BMC Evolutionary Biology* **13**: 1–11.
- Ding WN, Ree RH, Spicer RA, Xing YW. 2020. Ancient orogenic and monsoon-driven assembly of the world's richest temperate alpine flora. *Science* **369**: 578–581.
- Dixon P. 2003. VEGAN, a package of R functions for community ecology. *Journal of Vegetation Science* **14**: 927–930.
- Donoghue MJ. 2008. A phylogenetic perspective on the distribution of plant diversity. *Proceedings of the National Academy of Sciences, USA* **105**: 11549–11555.
- Donoghue MJ, Edwards EJ. 2014. Biome shifts and niche evolution in plants. *Annual Review of Ecology, Evolution, and Systematics* **45**: 547–572.
- Dupin J, Matzke NJ, Särkinen T, Knapp S, Olmstead RG, Bohs L, Smith SD. 2016. Bayesian estimation of the global biogeographical history of the Solanaceae. *Journal of Biogeography* **44**: 887–899.
- Edwards EJ, Chatelet DS, Chen BC, Ong JY, Tagane S, Kanemitsu H, Tagawa K, Teramoto K, Park B, Chung KF *et al.* 2017. Convergence, consilience, and the evolution of temperate deciduous forests. *The American Naturalist* **190**: S87–S104.
- Feeley KJ, Stroud JT. 2018. Where on Earth are the “tropics”? *Frontiers of Biogeography* **10**: e38649.
- Fick SE, Hijmans RJ. 2017. WORLDCLIM 2: new 1-km spatial resolution climate surfaces for global land areas. *International Journal of Climatology* **37**: 4302–4315.
- FitzJohn RG. 2012. DIVERSITREE: comparative phylogenetic analyses of diversification in R. *Methods in Ecology and Evolution* **3**: 1084–1092.

- Folk RA, Kates HR, LaFrance R, Soltis DE, Soltis PS, Guralnick RP. 2021. High-throughput methods for efficiently building massive phylogenies from natural history collections. *Applications in Plant Sciences* 9: e11410.
- Folk RA, Siniscalchi CM, Soltis DE. 2020. Angiosperms at the edge: extremity, diversity, and phylogeny. *Plant, Cell & Environment* 43: 2871–2893.
- Folk RA, Stubbs RL, Mort ME, Cellinese N, Allen JM, Soltis PS, Soltis DE, Guralnick RP. 2019. Rates of niche and phenotype evolution lag behind diversification in a temperate radiation. *Proceedings of the National Academy of Sciences, USA* 116: 10874–10882.
- Fu XG, Liu SY, van Velzen R, Stull GW, Tian Q, Li YX, Folk RA, Guralnick RP, Kates HR, Jin JJ *et al.* 2022. Phylogenomic analysis of the hemp family (Cannabaceae) reveals deep cyto-nuclear discordance and provides new insights into generic relationships. *Journal of Systematics and Evolution* 61: 806–826.
- Getis A, Ord JK. 1996. Spatial analysis and modeling in a GIS environment. In: McMaster RB, Userly EL, eds. *A research agenda for geographic information science*. Boca Raton, FL, USA: CRC Press, 157–196.
- Goldberg EE, Lancaster LT, Ree RH. 2011. Phylogenetic inference of reciprocal effects between geographic range evolution and diversification. *Systematic Biology* 60: 451–465.
- Goldblatt P, Savolainen V, Porteous O, Sostaric I, Powell M, Reeves G, Manning JC, Barraclough TG, Chase MW. 2002. Radiation in the Cape flora and the phylogeny of peacock irises *Moraea* (Iridaceae) based on four plastid DNA regions. *Molecular Phylogenetics and Evolution* 25: 341–360.
- Guzman B, Lledo MD, Vargas P. 2009. Adaptive radiation in Mediterranean *Cistus* (Cistaceae). *PLoS ONE* 4: e6362.
- Hauenschild F, Matuszak S, Muellner-Riehl AN, Favre A. 2016. Phylogenetic relationships within the cosmopolitan buckthorn family (Rhamnaceae) support the resurrection of *Sarcomphalus* and the description of *Pseudoziziphus* gen. nov. *Taxon* 65: 47–64.
- Hillebrand H. 2004. On the generality of the latitudinal diversity gradient. *The American Naturalist* 163: 192–211.
- Hopper SD. 2009. OCBIL theory: towards an integrated understanding of the evolution, ecology and conservation of biodiversity on old, climatically buffered, infertile landscapes. *Plant and Soil* 322: 49–86.
- Hughes CE. 2017. Are there many different routes to becoming a global biodiversity hotspot? *Proceedings of the National Academy of Sciences, USA* 114: 4275–4277.
- Igea J, Tanentzap AJ. 2019. Multiple macroevolutionary routes to becoming a biodiversity hotspot. *Science Advances* 5: eaau8067.
- Jablonski D, Roy K, Valentine JW. 2006. Out of the tropics: evolutionary dynamics of the latitudinal diversity gradient. *Science* 314: 102–106.
- Johnson MG, Gardner EM, Liu Y, Medina R, Goffinet B, Shaw AJ, Zerega NJ, Wickert NJ. 2016. HYBPIPER: extracting coding sequence and introns for phylogenetics from high-throughput sequencing reads using target enrichment. *Applications in Plant Sciences* 4: 1600016.
- Junier T, Zdobnov EM. 2010. The Newick utilities: high-throughput phylogenetic tree processing in the UNIX shell. *Bioinformatics* 26: 1669–1670.
- Katoh K, Standley DM. 2013. MAFFT multiple sequence alignment software v.7: improvements in performance and usability. *Molecular Biology and Evolution* 30: 772–780.
- Kellermann J. 2020. A preliminary survey of the leaf-indumentum in the Australian Pomaderreae (Rhamnaceae) using scanning electron microscopy. *Swainsona* 33: 75–102.
- Kembel SW, Cowan PD, Helmus MR, Cornwell WK, Morlon H, Ackerly DD, Blomberg SP, Webb CO. 2010. PICANTE: R tools for integrating phylogenies and ecology. *Bioinformatics* 26: 1463–1464.
- Kendall DG. 1949. Stochastic processes and population growth. *Journal of the Royal Statistical Society. Series B (Methodological)* 11: 230–282.
- Ladiges PY, Kellermann J, Nelson G, Humphries CJ, Udovicic F. 2005. Historical biogeography of Australian Rhamnaceae, tribe Pomaderreae. *Journal of Biogeography* 32: 1909–1919.
- Li HT, Luo Y, Gan L, Ma PF, Gao LM, Yang JB, Cai J, Gitzendanner MA, Fritsch PW, Zhang T *et al.* 2021. Plastid phylogenomic insights into relationships of all flowering plant families. *BMC Biology* 19: 1–13.
- Linder HP. 2003. The radiation of the Cape flora, southern Africa. *Biological Reviews* 78: 597–638.
- López-Pujol J, Zhang F-M, Sun H-Q, Ying T-S, Ge S. 2011. Centres of plant endemism in China: places for survival or for speciation? *Journal of Biogeography* 38: 1267–1280.
- Louca S, Pennell MW. 2020. Extant timetrees are consistent with a myriad of diversification histories. *Nature* 580: 502–505.
- Lu LM, Mao LF, Yang T, Ye JF, Liu B, Li HL, Sun M, Miller JT, Mathews S, Hu HH *et al.* 2018. Evolutionary history of the angiosperm flora of China. *Nature* 554: 234–238.
- Matzke NJ. 2013. Probabilistic historical biogeography: new models for founder-event speciation, imperfect detection, and fossils allow improved accuracy and model-testing. *Frontiers of Biogeography* 5: 242–248.
- Matzke NJ. 2014. Model selection in historical biogeography reveals that founder-event speciation is a crucial process in island clades. *Systematic Biology* 63: 951–970.
- Maurin KJL. 2020. An empirical guide for producing a dated phylogeny with TREEPL in a maximum likelihood framework. *arXiv*: 2008.07054.
- Medan D, Schirarend C. 2004. Rhamnaceae. In: Kubitzki K, ed. *Flowering plants. Dicotyledons: Celastrales, Oxalidales, Rosales, Cornales, Ericales*. Berlin, Heidelberg, Germany: Springer, 320–338.
- Mittelbach GG, Schemske DW, Cornell HV, Allen AP, Brown JM, Bush MB, Harrison SP, Hurlbert AH, Knowlton N, Lessios HA *et al.* 2007. Evolution and the latitudinal diversity gradient: speciation, extinction and biogeography. *Ecology Letters* 10: 315–331.
- Moran PAP. 1950. Estimation methods for evolutive processes. *Journal of the Royal Statistical Society. Series B (Methodological)* 13: 141–146.
- Morley RJ. 2000. *Origin and evolution of tropical rain forests*. Chichester, UK: Wiley.
- Myers N, Mittermeier RA, Mittermeier CG, da Fonseca GAB, Kent J. 2000. Biodiversity hotspots for conservation priorities. *Nature* 403: 853–858.
- Nge FJ, Kellermann J, Biffin E, Waycott M, Thiele KR. 2021. Historical biogeography of *Pomaderris* (Rhamnaceae): continental vicariance in Australia and repeated independent dispersals to New Zealand. *Molecular Phylogenetics and Evolution* 158: 107085.
- Onstein RE, Carter RJ, Xing Y, Richardson JE, Linder HP. 2015. Do Mediterranean-type ecosystems have a common history? – insights from the buckthorn family (Rhamnaceae). *Evolution* 69: 756–771.
- Onstein RE, Linder HP, Cornelissen H. 2016. Beyond climate: convergence in fast evolving sclerophylls in Cape and Australian Rhamnaceae predates the Mediterranean climate. *Journal of Ecology* 104: 665–677.
- Orr MC, Hughes AC, Chesters D, Pickering J, Zhu CD, Ascher JS. 2021. Global patterns and drivers of bee distribution. *Current Biology* 31: 451–458.
- Owens HL, Lewis DS, Dupuis JR, Clamens AL, Sperling FAH, Kawahara AY, Guralnick RP, Condamine FL, Kerr J. 2017. The latitudinal diversity gradient in New World swallowtail butterflies is caused by contrasting patterns of out-of- and into-the-tropics dispersal. *Global Ecology and Biogeography* 26: 1447–1458.
- Oxoli D, Prestifilippo G, Bertocchi D. 2017. Enabling spatial autocorrelation mapping in QGIS: the hotspot analysis Plugin. *Geoinformatica Ambientale e Mineraria* 151: 45–50.
- Palazzesi L, Hidalgo O, Barreda VD, Forest F, Hohna S. 2022. The rise of grasslands is linked to atmospheric CO<sub>2</sub> decline in the late Palaeogene. *Nature Communications* 13: 1–10.
- Paradis E, Claude J, Strimmer K. 2004. APE: analyses of phylogenetics and evolution in R language. *Bioinformatics* 20: 289–290.
- Peel MC, Finlayson BL, McMahon TA. 2007. Updated world map of the Köppen-Geiger climate classification. *Hydrology and Earth System Sciences* 11: 1633–1644.
- Pennington RT, Lavin M. 2016. The contrasting nature of woody plant species in different neotropical forest biomes reflects differences in ecological stability. *New Phytologist* 210: 25–37.
- Pontarp M, Bunnefeld L, Cabral JS, Etienne RS, Fritz SA, Gillespie R, Graham CH, Hagen O, Hartig F, Huang S *et al.* 2019. The latitudinal diversity gradient: novel understanding through mechanistic eco-evolutionary models. *Trends in Ecology & Evolution* 34: 211–223.
- QGIS Development Team. 2018. *QGIS geographic information system*. Oregon, USA: Open Source Geospatial Foundation Project. [WWW document] URL <http://qgis.osgeo.org> [accessed 8 April 2022].

- R Core Team. 2022. *R: a language and environment for statistical computing*. Vienna, Austria: R foundation for Statistical Computing. [WWW document] URL <http://www.r-project.org> [accessed 8 April 2022].
- Renner MAM, Foster CSP, Miller JT, Murphy DJ. 2020. Increased diversification rates are coupled with higher rates of climate space exploration in Australian *Acacia* (Caesalpinioideae). *New Phytologist* 226: 609–622.
- Richardson JE, Fay MF, Cronk QCB, Bowman D, Chase MW. 2000a. A phylogenetic analysis of Rhamnaceae using *rbcL* and *trnL-F* plastid DNA sequences. *American Journal of Botany* 87: 1309–1324.
- Richardson JE, Fay MF, Cronk QCB, Chase MW. 2000b. A revision of the tribal classification of Rhamnaceae. *Kew Bulletin* 55: 311–340.
- Richardson JE, Weitz FM, Fay MF, Cronk QCB, Linder HP, Reeves G, Chase MW. 2001. Phylogenetic analysis of *Phyllica* L. (Rhamnaceae) with an emphasis on island species: evidence from plastid *trnL-F* DNA and nuclear internal transcribed spacer (ribosomal DNA) sequences. *Taxon* 50: 405–427.
- Rundel PW, Arroyo MTK, Cowling RM, Keeley JE, Lamont BB, Vargas P. 2016. Mediterranean biomes: evolution of their vegetation, floras, and climate. *Annual Review of Ecology, Evolution, and Systematics* 47: 383–407.
- Schluter D, Pennell MW. 2017. Speciation gradients and the distribution of biodiversity. *Nature* 546: 48–55.
- Simpson GG. 1953. *The major features of evolution*. New York, NY, USA: Columbia University Press.
- Skeels A. 2019. Lineages through space and time plots: visualising spatial and temporal changes in diversity. *Frontiers of Biogeography* 11: e42954.
- Slater GS, Birney E. 2005. Automated generation of heuristics for biological sequence comparison. *BMC Bioinformatics* 6: 1–11.
- Smith SA, O'Meara BC. 2012. TREEPL: divergence time estimation using penalized likelihood for large phylogenies. *Bioinformatics* 28: 2689–2690.
- Soltis PS, Folk RA, Soltis DE. 2019. Darwin review: angiosperm phylogeny and evolutionary radiations. *Proceedings of the Royal Society B: Biological Sciences* 286: 20190099.
- Sosa V, De-Nova JA, Vásquez-Cruz M. 2018. Evolutionary history of the flora of Mexico: dry forests cradles and museums of endemism. *Journal of Systematics and Evolution* 56: 523–536.
- Spriggs EL, Christin PA, Edwards EJ. 2014. C<sub>4</sub> photosynthesis promoted species diversification during the Miocene grassland expansion. *PLoS ONE* 9: e97722.
- Stamatakis A. 2014. RAxML v.8: a tool for phylogenetic analysis and post-analysis of large phylogenies. *Bioinformatics* 30: 1312–1313.
- Stebbins GL, Major J. 1965. Endemism and speciation in the California flora. *Ecological Monographs* 35: 2–35.
- Stephens PR, Wiens JJ. 2003. Explaining species richness from continents to communities: the time-for-speciation effect in emydid turtles. *The American Naturalist* 161: 112–128.
- Stroud JT, Losos JB. 2016. Ecological opportunity and adaptive radiation. *Annual Review of Ecology, Evolution, and Systematics* 47: 507–532.
- Suissa JS, Sundue MA, Testo WL. 2021. Mountains, climate and niche heterogeneity explain global patterns of fern diversity. *Journal of Biogeography* 48: 1296–1308.
- Sun M, Folk RA, Gitzendanner MA, Soltis PS, Chen Z, Soltis DE, Guralnick RP. 2020. Recent accelerated diversification in rosids occurred outside the tropics. *Nature Communications* 11: 3333.
- Thompson JB, Davis KE, Dodd HO, Wills MA, Priest NK. 2023a. Speciation across the Earth driven by global cooling in terrestrial orchids. *Proceedings of the National Academy of Sciences, USA* 120: e2102408120.
- Thompson JB, Ramirez-Barahona S, Priest N, Hernández-Hernández T. 2023b. Did succulents diversify in response to aridity? Evolutionary analyses of major succulent lineages around the world. *bioRxiv*. doi: 10.1101/2023.05.23.541957.
- Valente LM, Savolainen V, Vargas P. 2010. Unparalleled rates of species diversification in Europe. *Proceedings of the Royal Society B: Biological Sciences* 277: 1489–1496.
- Wang Q, Huang J, Zang R, Li Z, El-Kassaby YA. 2022. Centres of neo- and paleo-endemism for Chinese woody flora and their environmental features. *Biological Conservation* 276: 109817.
- Webb CO, Ackerly DD, McPeck MA, Donoghue MJ. 2002. Phylogenies and community ecology. *Annual Review of Ecology and Systematics* 33: 475–505.
- Wiens JJ, Donoghue MJ. 2004. Historical biogeography, ecology and species richness. *Trends in Ecology and Evolution* 19: 639–644.
- Xing Y, Onstein RE, Carter RJ, Stadler T, Linder PH. 2014. Fossils and a large molecular phylogeny show that the evolution of species richness, generic diversity, and turnover rates are disconnected. *Evolution* 68: 2821–2832.
- Xing Y, Ree RH. 2017. Uplift-driven diversification in the Hengduan Mountains, a temperate biodiversity hotspot. *Proceedings of the National Academy of Sciences, USA* 114: E3444–E3451.
- Yan HF, Zhang CY, Anderberg AA, Hao G, Ge XJ, Wiens JJ. 2018. What explains high plant richness in East Asia? Time and diversification in the tribe Lysimachieae (Primulaceae). *New Phytologist* 219: 436–448.
- Zachos J, Pagani M, Sloan L, Thomas E, Billups K. 2001. Trends, rhythms, and aberrations in global climate 65 Ma to present. *Science* 292: 686–693.
- Zanne AE, Pearse WD, Cornwell WK, McGlenn DJ, Wright IJ, Uyeda JC. 2018. Functional biogeography of angiosperms: life at the extremes. *New Phytologist* 218: 1697–1709.
- Zhang C, Rabiee M, Sayyari E, Mirarab S. 2018. ASTRAL-III: polynomial time species tree reconstruction from partially resolved gene trees. *BMC Bioinformatics* 19: 15–30.
- Zhang X, Landis JB, Sun Y, Zhang H, Lin N, Kuang T, Huang X, Deng T, Wang H, Sun H. 2021. Macroevolutionary pattern of *Saussurea* (Asteraceae) provides insights into the drivers of radiating diversification. *Proceedings of the Royal Society B: Biological Sciences* 288: 20211575.
- Zhang XX, Ye JF, Laffan SW, Mishler BD, Thornhill AH, Lu LM, Mao LF, Liu B, Chen YH, Lu AM *et al.* 2022. Spatial phylogenetics of the Chinese angiosperm flora provides insights into endemism and conservation. *Journal of Integrative Plant Biology* 64: 105–117.

## Supporting Information

Additional Supporting Information may be found online in the Supporting Information section at the end of the article.

**Dataset S1** Sampled species and collection information of Rhamnaceae and outgroups.

**Dataset S2** Concatenated alignment supermatrix of 89 low-copy loci of Rhamnaceae and outgroups.

**Dataset S3** Occurrence data of 1022 Rhamnaceae species from GBIF.

**Dataset S4** Information of species richness, 35 climatic variables, and classification as temperate vs tropical biomes within each grid cell of 1° × 1°.

**Dataset S5** Classification information of the temperate vs tropical biomes for 1022 Rhamnaceae species.

**Fig. S1** Maximum likelihood (ML) tree of Rhamnaceae and outgroups inferred by RAxML based on the concatenated supermatrix of 89 low-copy loci under an unpartitioned GTR-GAMMA model.

**Fig. S2** Species tree of Rhamnaceae and outgroups inferred by ASTRAL-III based on 89 low-copy gene trees.

**Fig. S3** Divergence times of Rhamnaceae estimated from the concatenated supermatrix of 89 low-copy loci using TREEPL.

**Fig. S4** Seven diversification hotspots of Rhamnaceae identified based on species richness using the  $G_i^*$  local statistic implemented in QGIS v.3.2.

**Fig. S5** Occupancy and biplot of hypervolume environmental space in Rhamnaceae climatic-based temperate and tropical biomes and each diversification hotspot.

**Fig. S6** Ancestral range reconstruction and per-area probabilities of Rhamnaceae hotspots under the BAYAREALIKE + J model using BioGeoBEARS.

**Fig. S7** Ancestral range reconstruction and per-area probabilities of Rhamnaceae buffer hotspots under the BAYAREALIKE model using BioGeoBEARS.

**Fig. S8** Lineage through time (LTT) across each Rhamnaceae hotspot and nonhotspot regions using biogeographical stochastic mappings (BSMs) analysis.

**Fig. S9** Diversification rates across climatic-based temperate and tropical biomes and each buffer hotspot in Rhamnaceae.

**Fig. S10** Source and sink dynamics of Rhamnaceae in climatic-based temperate biomes and each buffer hotspot.

**Fig. S11** Ancestral state estimates and per-state probabilities of Rhamnaceae geographic-based temperate and tropical biomes from the best-fitting GeoSSE model.

**Fig. S12** Ancestral state estimates and per-state probabilities of Rhamnaceae climatic-based temperate and tropical biomes from the best-fitting GeoSSE model.

**Fig. S13** Global pattern of Rhamnaceae net relatedness index (NRI) plotted in grid cells of  $1^\circ \times 1^\circ$ .

**Methods S1** Description and placement of fossil calibrations for divergence time estimation of Rhamnaceae.

**Table S1** Overlap percentage of climatic hypervolumes among seven hotspots in Rhamnaceae.

**Table S2** Model testing in Rhamnaceae BioGeoBEARS analysis.

**Table S3** Model testing in Rhamnaceae GeoSSE analysis.

Please note: Wiley is not responsible for the content or functionality of any Supporting Information supplied by the authors. Any queries (other than missing material) should be directed to the *New Phytologist* Central Office.